

# Enhancement of the External Quantum Efficiency of a Silicon Quantum Dot Light-Emitting Diode by Localized Surface Plasmons\*\*

By Beak-Hyun Kim, Chang-Hee Cho, Jin-Soo Mun, Min-Ki Kwon, Tae-Young Park, Jong Su Kim, Clare Chisu Byeon, Jongmin Lee, and Seong-Ju Park\*

Effective light emission from low-dimensional silicon materials such as porous silicon, silicon nanocrystals, and superlattices has been demonstrated at room temperature in spite of the indirect bandgap nature of bulk silicon.<sup>[1–5]</sup> In particular, silicon quantum dot (Si QD) light-emitting diodes (LEDs) have recently been investigated as a promising light source for the next generation of optical interconnections.<sup>[6–8]</sup> However, the quest for highly efficient Si QD LEDs remains unfulfilled. To achieve this goal, new LED structures are being developed to enhance the external quantum efficiency ( $\eta_{\text{ext}}$ ), which is a product of the light-extraction efficiency ( $\eta_{\text{extraction}}$ ), radiative efficiency ( $\eta_{\text{rad}}$ ), and current-injection efficiency ( $\eta_{\text{inj}}$ ).<sup>[9]</sup> Among the new approaches, increasing the radiative recombination rate by coupling QDs to surface plasmons (SPs, collective charge oscillations at the interface between a metal and a dielectric material) has attracted a great deal of attention.<sup>[10–12]</sup> Although enhanced photoluminescence (PL) of SP-coupled nanostructures such as QDs<sup>[13–17]</sup> and quantum wells (QWs)<sup>[18]</sup> has been reported, there has been no report concerning the enhancement of electroluminescence (EL) in Si QD LEDs through a Si QD–SP coupling effect. Here, we show the first evidence of enhanced  $\eta_{\text{ext}}$  in a Si QD LED resulting from the coupling between Si QDs and localized surface plasmons (LSPs) and effective current tunneling into Si QDs from an Ag layer containing Ag particles inserted between the Si QD layer and Si substrate.

Surface plasmon excitations in bounded geometries, such as nanostructured metallic particles, are LSPs. The resonant excitation of LSPs on the surface of nanostructured metallic particles by an incident electromagnetic field (light) causes strong light scattering and absorption, and enhanced local electromagnetic fields. LSPs are generally used in many

applications such as ultrafast switches, optical tweezers, labeling biomolecules, optical filters, biosensors, surface-enhanced spectroscopies, plasmonics, and chemical sensors.<sup>[19–22]</sup> SPs are evanescent waves that exponentially decay with distance from a metal surface. Si QDs located within the near-field of the metal surface can be effectively coupled to SP mode.<sup>[13,18,19]</sup> In order to keep the close distance between Si QDs and the metal layer for Si QD–LSP coupling, we propose a Si QD LED structure with an Ag layer containing Ag particles inserted between the silicon nitride layer containing Si QDs and the Si substrate layer, as shown in Figure 1.

Figure 2a and b shows cross-sectional transmission electron microscopy (TEM) images of Si QD LEDs with and without an Ag layer. Figure 2a depicts the interface between the silicon nitride and Si substrate of a reference Si QD LED. Figure 2b is an image of the interfaces between the silicon nitride layer, Ag layer, and the Si substrate. The silicon nitride film deposited on the Ag layer was similar in thickness to the silicon nitride layer in the reference Si QD LED. The TEM image of the Si QD LED with an Ag layer in Figure 2b indicates that the Ag layer consists of Ag particles. The average height and diameter of Ag particles deposited on a Si substrate were measured to be  $8 \pm 2$  nm and  $98 \pm 59$  nm, respectively, by using atomic force microscopy (AFM) analysis. The average Ag particle height was in good agreement with the thickness of the Ag layer in the TEM image of Figure 2b. This result indicates that the surface of Ag layer is rougher than that of the flat Si substrate owing to the formation of Ag particles. To check the atomic mixing at the silicon-nitride/Si and Ag/silicon-nitride interfaces, depth profile analyses of Si QD LEDs were performed by using the Si 2p, N 1s, and Ag 3d peaks from X-ray photoelectron spectroscopy (XPS). The results, depicted in Figure 2c, indicate that atomic intermixing between the silicon nitride layer and the silicon substrate did not occur in the reference Si QD LED. Figure 2d demonstrates that in the device containing an Ag layer, Ag atoms did not diffuse into the silicon nitride.

To understand the effect of the Ag layer on PL emission in Si QD LEDs, PL spectra of Si QD layers with and without an Ag layer were measured at room temperature, as shown in Figure 3a. The average size of the Si QDs (3.78 nm) was estimated from the band gap of Si QDs using the relationship  $E(\text{eV}) = 1.13 + 13.9/a^2$ ,<sup>[23]</sup> where  $E$  and  $a$  are the energy band gap measured from the PL peak position and the diameter of Si QDs, respectively. Figure 3b shows a plot of the PL

[\*] Prof. S.-J. Park, B.-H. Kim, C.-H. Cho, J.-S. Mun, M.-K. Kwon, T.-Y. Park  
Department of Materials Science and Engineering  
Gwangju Institute of Science and Technology  
Gwangju 500-712 (Korea)  
E-mail: sjpark@gist.ac.kr

Dr. J. S. Kim, Dr. C. C. Byeon, Prof. J. Lee  
Advanced Photonics Research Institute  
Gwangju Institute of Science and Technology  
Gwangju 500-712 (Korea)

[\*\*] This work was supported by a Korea Science and Engineering Foundation (KOSEF) grant funded by the Korean government (MOST) (No. R17-2007-078-01000-0) and the Brain Korea 21 program.

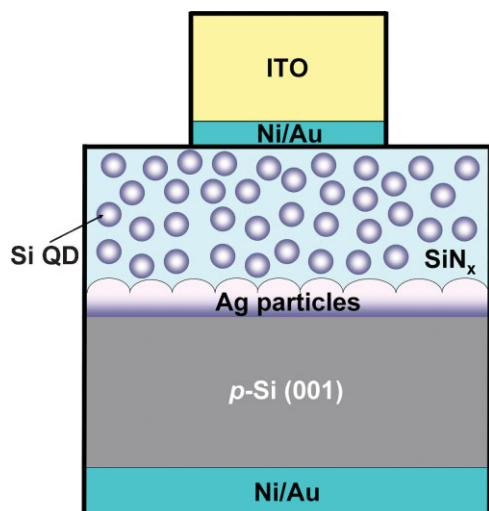


**Figure 1.** Schematic diagram of a Si QD LED with an Ag layer containing Ag particles. The SiN<sub>x</sub> film contains Si QDs.

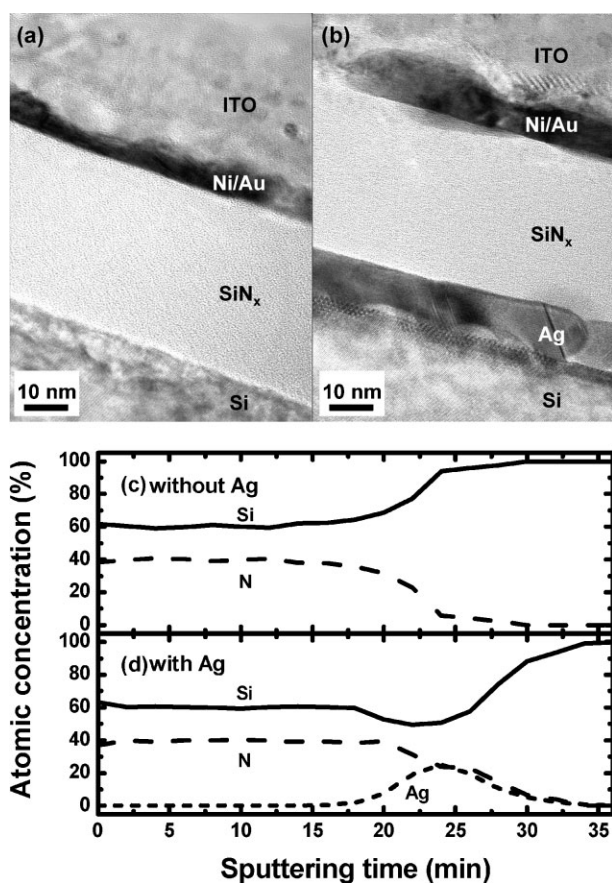


**Figure 2.** Cross-sectional TEM images of a) a reference Si QD LED, and b) a Si QD LED with an Ag layer. The Si QD layer is a SiN<sub>x</sub> film containing Si QDs. X-ray photoelectron spectroscopy (XPS) depth profiles for Si, N, and Ag elements in c) the reference Si QD LED and d) the Si QD LED with an Ag layer.

enhancement factor,  $I_{\text{Ag}}(\lambda)/I_{\text{ref}}(\lambda)$  where  $I_{\text{Ag}}(\lambda)$ , and  $I_{\text{ref}}(\lambda)$  are PL intensities for the Si QD layers with and without an Ag layer. A maximum PL enhancement factor of 1.93 was observed at 530 nm, as shown in Figure 3b. Figure 3c shows absorption spectra of (i) SiN<sub>x</sub>/Ag/Si, (ii) Ag/SiN<sub>x</sub>, (iii) Si, and (iv) SiN<sub>x</sub> layered structures on glass substrates. The absorbance of the SiN<sub>x</sub>/Ag/Si layered structure is rapidly increased from 450 nm to the high-energy-side owing to the absorbance of the 20 nm thick Si layer and the SiN<sub>x</sub> layer containing Si QDs, as shown in Figure 3c. Absorption spectra of SiN<sub>x</sub>/Ag/Si and Ag/SiN<sub>x</sub> layered structures show the nearly same maximum absorption peaks at 535 nm and 538 nm, respectively. These maximum absorption peaks are due to the change of SP resonance energies by localized SPs in Ag particles,<sup>[24–27]</sup> which are evidenced by TEM and AFM analyses. The PL enhancement band may shift because the light generated at the interface between Si QD layer and Ag layer is reabsorbed and re-emitted in upper Si QDs. However, this possibility was excluded owing to the low absorbance of the Si QD layer in the visible range, as shown in Figure 3c. Therefore, the similar peak positions of PL enhancement factor and absorption strongly indicate that the maximum PL enhancement factor of 1.93 is attributed to Si QD–LSP coupling due to charge density oscillations of confined SP modes in the Ag layer containing Ag particles. The radiative recombination rate ( $\Gamma_{\text{rad}}$ ) for exciton dipoles of Si QDs is given by Fermi's golden rule,  $\Gamma_{\text{rad}} = \frac{2\pi}{\hbar} \rho | \langle f | \mu \cdot \mathbf{E} | i \rangle |^2$ ,<sup>[28]</sup> where  $\rho$  is the photon density of states and  $\langle f | \mu \cdot \mathbf{E} | i \rangle$  is the matrix element for the interaction. When exciton dipole moments ( $\mu$ ) of Si QDs strongly couple to the local electric field ( $E$ ) of LSPs in Ag layer, the Si QD–LSP coupling increases the  $\Gamma_{\text{rad}}$ , resulting in an increase in  $\eta_{\text{rad}}$ . To further confirm that the large PL enhancement factor is not due to the increase of reflectance of the Ag layer or the surface roughness of the Si QD layers, the change of reflectance and surface roughness of Si QD LED with and without the Ag layer were measured. The reflectance change resulting from addition of the Ag layer was measured by comparing the reflectance of a 10 nm thick Ag layer deposited on a silicon substrate to that of a bare silicon substrate as shown in Figure 3d. Deposition of an Ag layer increased the reflectance at 530 nm by only 8.6%. Another possible explanation for the PL enhancement factor would be an increase in the surface roughness of the Si QD layer, since increased surface roughness may lead to increased light extraction. The root mean square (RMS) surface roughness of a Si QD layer on an Ag layer was 2.25 nm, while a Si QD layer grown directly on the Si substrate had a roughness of 2.45 nm. Therefore, these results strongly suggest that the PL enhancement factor of 1.93 at 530 nm observed in Figure 3b is not due to the slight increase in reflectance from the Ag layer or to the surface roughness of the Si QD layer. We also prepared a single sample of silicon nitride film containing Si QDs on the sapphire substrate and covered half of it with an Ag layer to measure the PL and absorption spectrum in order to avoid any artifacts due to different Si QD concentration. The results were in good agreement with those of Si QD LED with and without an Ag layer shown in Figure 3, suggesting that the

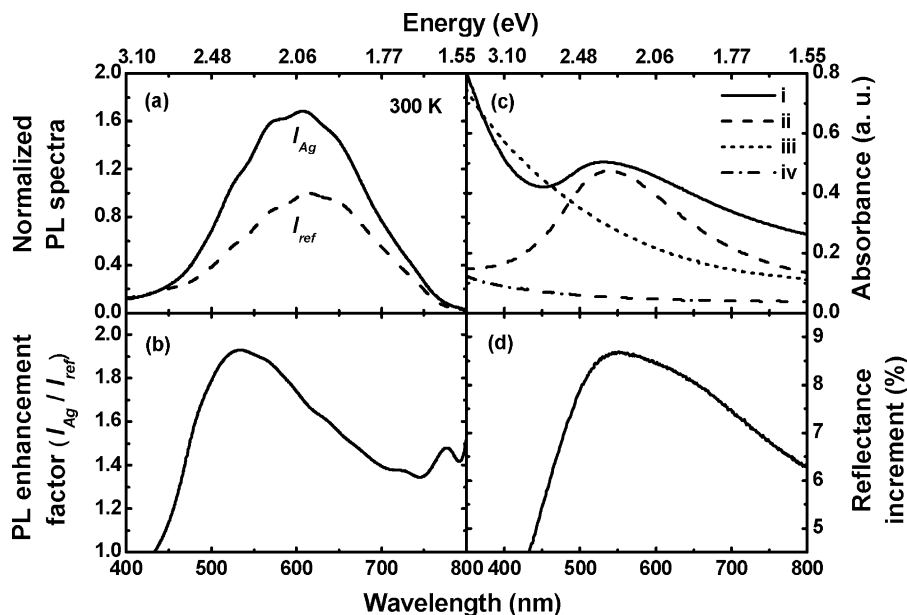


**Figure 3.** a) Normalized PL spectra of Si QD layers with an Ag layer (top curve) and without an Ag layer (bottom curve) at room temperature. b) PL enhancement factor (PL intensity ratio of samples in (a)). c) Absorbance of (i) SiN<sub>x</sub>/Ag/Si, (ii) Ag/SiN<sub>x</sub>, (iii) Si, and (iv) SiN<sub>x</sub> layered structures. d) Reflectance increment of the Ag layer. The SiN<sub>x</sub> films contain Si QDs.

Ag layer did not influence the Si QD concentration in the Si QD LED. Therefore, the PL enhancement factor shown in Figure 3b was attributed to the enhanced  $\eta_{\text{rad}}$  of Si QDs due to Si QD-LSP coupling.<sup>[13,14,29]</sup>

The EL spectra of Si QD LEDs with and without an Ag layer were measured as a function of injection current, as shown in Figure 4a and b. Figure 4c depicts the integrated EL intensities of Si QD LEDs with and without the Ag layer in the visible region as a function of injection current. The integrated EL intensities of the Si QD LEDs with and without the Ag layer increased with increasing current. Figure 4d shows a graph of the EL enhancement, which is the ratio of integrated EL intensities of Si QD LEDs with and without the Ag layer, as a function of injection current. To understand the EL enhancement in Figure 4d, the EL enhancement factor,  $I_{\text{Ag}}(\lambda)/I_{\text{ref}}(\lambda)$  as a function of injection current, was measured as shown in Figure 4e.  $I_{\text{Ag}}(\lambda)$  and  $I_{\text{ref}}(\lambda)$  are the EL intensities from Si QD LEDs with and without an Ag layer as shown in Figure 4a and b. A maximum EL enhancement factor of 4.34 was observed at 538 nm at a current of 20 mA as shown in Figure 4e. The wavelength of maximum EL enhancement factor at a current of 20 mA is very close to that of maximum PL enhancement factor as shown in Figure 3b, indicating that the PL and EL enhancement factors originate from the same source of Si QD-LSP coupling. Figure 4d also shows that the maximum EL enhancement of 3.2 was observed at a current of 20 mA and the EL enhancement was rapidly decreased until leveling off at approximately 2.0 as the current approached 40 mA. This result can be explained by the screening effect of excess charges in Si QDs with increasing current, resulting in a

decrease of exciton dipole coupling with LSPs as shown in Figure 4e. To further understand the observed EL enhancement in Figure 4d, the current–voltage ( $I$ – $V$ ) characteristics of Si QD LEDs with and without the Ag layer were compared as shown in Figure 4f. The threshold voltage was 9.1 V for a Si QD LED with an Ag layer and 14.2 V for the reference Si QD LED. The low threshold voltage indicates that addition of an Ag layer significantly enhances the carrier injection into Si QDs. The increase in carrier injection is attributed to the rough surface of the Ag layer containing Ag particles, which enhances the inhomogeneous local electric fields at the interface between the Ag layer and the silicon nitride matrix.<sup>[30–32]</sup> The enhanced inhomogeneous local electric fields can increase the tunneling probability of carriers into Si QDs through the silicon nitride. Therefore, an Ag layer is believed to greatly increase  $\eta_{\text{inj}}$  in Si QD LEDs. The EL enhancement factor in Figure 4e is also much larger compared to the PL enhancement factor of 1.93 as shown in Figure 3b. The large EL enhancement factor is due to the enhancement of  $\eta_{\text{inj}}$  by the effective tunneling of carriers into Si QDs. These results indicate that the significant EL enhancement can be attributed to an increase in  $\eta_{\text{ext}}$  due to Si QD-LSP coupling and an effective carrier tunneling process by an Ag layer in Si QD LEDs.

We have demonstrated that the EL intensity of a Si QD LED with an Ag layer containing Ag particles can be enhanced by 434% relative to a Si QD LED without an Ag layer. The large EL enhancement was attributed to an increase in  $\eta_{\text{rad}}$  as a result of Si QD-LSP coupling and increased  $\eta_{\text{inj}}$  through improved carrier tunneling into Si QDs.

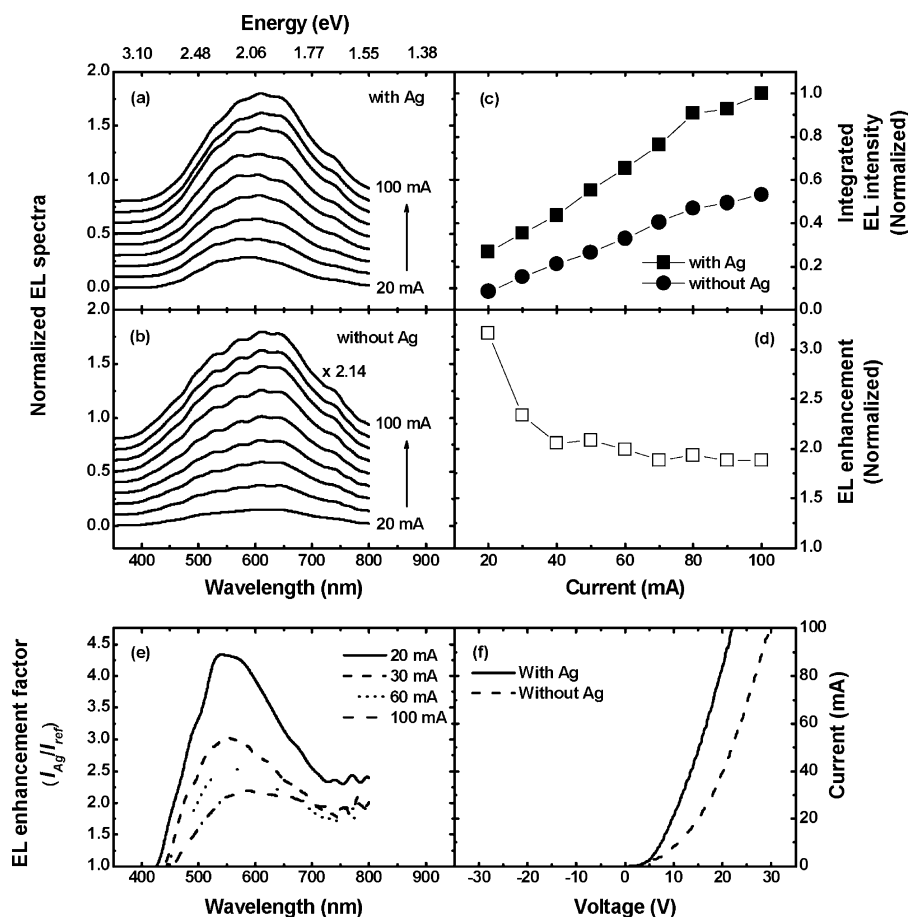


**Figure 4.** Normalized EL spectra of a) a Si QD LED with an Ag layer and b) a reference Si QD LED as a function of injection current. c) Integrated EL intensity in the visible range as a function of injection current. d) EL enhancement (EL intensity ratio of LEDs shown in (c)). e) EL enhancement factor (EL intensity ratio of EL spectra shown in (a) and (b)) as a function of injection current. f) I–V characteristics of Si QD LED with an Ag layer (solid line) and reference Si QD LED (dashed line).

## Experimental

**Fabrication:** To investigate the effect of an Ag layer containing Ag particles on the  $\eta_{ext}$  of a Si QD LED, we deposited a 10 nm thick Ag layer by e-beam evaporation on a *p*-type Si wafer (100) with a hole concentration of ca.  $10^{15} \text{ cm}^{-3}$ . A 37 nm thick amorphous silicon nitride film containing Si QDs was grown on the Ag layer by plasma-enhanced chemical vapor deposition (PECVD) using ammonia and nitrogen-diluted 5% silane as the reactant gas sources. The flow rates of ammonia and silane were 10 sccm and 190 sccm, respectively. The pressure, growth temperature, and plasma power were maintained at 1.0 Torr, 300 °C, and 10 W, respectively. To measure the absorbance of a Si QD layer over an Ag layer, Ag (10 nm) and Si (20 nm) layers were deposited on a glass substrate by e-beam evaporation, and a 37 nm thick  $\text{SiN}_x$  containing Si QDs was grown on the Ag/Si layers by PECVD. For comparison measurements, 20 nm thick Si and Ag/ $\text{SiN}_x$  layered structures on glass substrate were deposited. To measure the electrical and optical properties of Si QD LEDs containing an Ag layer, a transparent metal contact consisting of Ni (5 nm), Au (5 nm), and indium tin oxide (ITO, 100 nm) was deposited on the silicon nitride film by e-beam evaporation. To ensure transparency, the deposited ITO layer was annealed at 400 °C in the air and nitrogen atmospheres for 30 s, respectively. A Ni (20 nm)/Au (100 nm) contact was deposited on the backside of the Si substrate. For comparison measurements, a Si

QD LED without an Ag layer was also fabricated as a reference Si QD LED.

**Measurement:** A charge-coupled device was used for PL and EL spectral measurements at room temperature, using a He–Cd 325 nm laser as the excitation source for PL. The I–V characteristics of the LEDs were measured using an HP 4155A semiconductor parameter analyzer.

Received: December 11, 2007

Revised: March 15, 2008

Published online: June 16, 2008

- [1] L. T. Canham, *Appl. Phys. Lett.* **1990**, 57, 1046.
- [2] A. G. Cullis, L. T. Canham, *Nature* **1991**, 353, 335.
- [3] W. L. Wilson, P. F. Szajowski, L. E. Brus, *Science* **1993**, 262, 1242.
- [4] Z. H. Lu, D. J. Lockwood, J. M. Baribeau, *Nature* **1995**, 378, 258.
- [5] K. D. Hirschman, L. Tsybeskov, S. P. Duttagupta, P. M. Fauchet, *Nature* **1996**, 384, 338.
- [6] L. Pavesi, L. Dal Negro, C. Mazzoleni, G. Franzò, F. Priolo, *Nature* **2000**, 408, 440.
- [7] N. M. Park, T. S. Kim, S. J. Park, *Appl. Phys. Lett.* **2001**, 78, 2575.

- [8] B. H. Kim, C. H. Cho, N. M. Park, G. Y. Sung, S. J. Park, *Appl. Phys. Lett.* **2006**, 89, 063509.
- [9] A. Žukauskas, M. S. Shur, R. Gaska, *Introduction to Solid-State Lighting*, Wiley, New York **2002**.
- [10] H. Raether, *Surface Plasmons on Smooth and Rough Surfaces and on Gratings*, Springer, Berlin **1988**.
- [11] R. R. Chance, A. Prock, R. Silbey, *Adv. Chem. Phys.* **1978**, 37, 1.
- [12] G. W. Ford, W. H. Weber, *Phys. Rep.* **1984**, 113, 195.
- [13] J. S. Biteen, D. Pacifici, N. S. Lewis, H. A. Atwater, *Nano Lett.* **2005**, 5, 1768.
- [14] J. S. Biteen, N. S. Lewis, H. A. Atwater, H. Mertens, A. Polman, *Appl. Phys. Lett.* **2006**, 88, 131109.
- [15] J. Kalkman, H. Gersen, L. Kuipers, A. Polman, *Phys. Rev. B* **2006**, 73, 075317.
- [16] K. T. Shimizu, W. K. Woo, B. R. Fisher, H. J. Eisler, M. G. Bawendi, *Phys. Rev. Lett.* **2002**, 89, 117401.
- [17] O. Kulakovich, N. Strekal, A. Yaroshevich, S. Maskevich, S. Gaponenko, I. Nabiev, U. Woggon, M. Artemyev, *Nano Lett.* **2002**, 2, 1449.
- [18] K. Okamoto, I. Niki, A. Shvartser, Y. Narukawa, T. Mukai, A. Scherer, *Nat. Mater.* **2004**, 3, 601.
- [19] W. L. Barnes, A. Dereux, T. W. Ebbesen, *Nature* **2003**, 424, 824.
- [20] E. Hutter, J. H. Fendler, *Adv. Mater.* **2004**, 16, 1685.
- [21] W. A. Murray, W. L. Barnes, *Adv. Mater.* **2007**, 19, 3771.
- [22] S. A. Maier, *Plasmonics: Fundamentals and Applications*, Springer, New York **2007**.
- [23] T. W. Kim, B. H. Kim, C. H. Cho, S. J. Park, *Appl. Phys. Lett.* **2006**, 88, 123102.
- [24] W. A. Weimer, M. J. Dyer, *Appl. Phys. Lett.* **2001**, 79, 3164.
- [25] R. Gupta, M. J. Dyer, W. A. Weimer, *J. Appl. Phys.* **2002**, 92, 5264.
- [26] K. L. Kelly, E. Coronado, L. L. Zhao, G. C. Schatz, *J. Phys. Chem. B* **2003**, 107, 668–677.
- [27] G. Xu, M. Tazawa, P. Jin, S. Nakao, K. Yoshimura, *Appl. Phys. Lett.* **2003**, 82, 3811.
- [28] E. Fermi, *Rev. Mod. Phys.* **1932**, 4, 87.
- [29] J. Gersten, A. Nitzan, *J. Chem. Phys.* **1981**, 75, 1139.
- [30] R. T. Tung, *Phys. Rev. B* **1992**, 45, 13509.
- [31] Y. S. Kim, Y. H. Lee, K. M. Lim, M. Y. Sung, *Appl. Phys. Lett.* **1999**, 74, 2800.
- [32] N. Gaillard, L. Pinzelli, M. Gros-Jean, A. Bsiesy, *Appl. Phys. Lett.* **2006**, 89, 133506.